Anderson localization of light near boundaries of disordered photonic lattices

Dragana M. Jović,[1,2] Yuri S. Kivshar,[3] Cornelia Denz,[4] and Milivoj R. Belić[2]
[1]*Institute of Physics, P. O. Box 57, 11001 Belgrade, Serbia*
[2]*Texas A&M University at Qatar, P. O. Box 23874, Doha, Qatar*
[3]*Nonlinear Physics Center, Research School of Physics and Engineering, Australian National University, Canberra ACT 0200, Australia*
[4]*Institut für Angewandte Physik and Center for Nonlinear Science (CeNoS), Westfälische Wilhelms-Universität Münster, D-48149 Münster, Germany*
(Received 2 January 2011; published 10 March 2011)

We study numerically the effect of boundaries on Anderson localization of light in truncated two-dimensional photonic lattices in a nonlinear medium. We demonstrate suppression of Anderson localization at the edges and corners, so that stronger disorder is needed near the boundaries to obtain the same localization as in the bulk. We find that the level of suppression depends on the location in the lattice (edge vs corner), as well as on the strength of disorder. We also discuss the effect of nonlinearity on various regimes of Anderson localization.

DOI: 10.1103/PhysRevA.83.033813 PACS number(s): 42.65.Tg, 71.23.−k, 71.55.Jv

I. INTRODUCTION

Anderson localization has gained renewed interest due to the evident potential for the realization of localization of optical waves in random media [1]. It has become a central part of recent investigations of discrete, photonic, band-gap lattices with nonperiodic, i.e., random, structures. Owing to the analogy of these photonic systems to solid-state systems, and thanks to the fact that longitudinally invariant disorder is more easily realized in lattices, experimental activities in Anderson localization of light have recently taken a new turn [2,3]. Similar observations of Anderson localization have been made in other fields, for example in Bose-Einstein condensates [4]. These experiments motivated numerous theoretical studies, including the analysis of wave spreading in nonlinear disordered systems [5] and Anderson localization, and lasing in photonic crystals [6]. The concept of Anderson localization of light was introduced some time ago [7], but recently it has been extended to include the dynamical localization of mutually incoherent counterpropagating beams, in which time-dependent effects can take place [8].

Since wave localization in random structures relies on fluctuations imposed on an otherwise periodic structure, the truncation of the lattice yields an additional distortion in the periodicity and induces the formation of localized surface states. One would expect that the presence of boundaries in random lattices would enhance the localization. However, a recent experimental study of the light localization near the edge of a truncated one-dimensional (1D) photonic lattice revealed that boundaries can suppress the localization effects [9].

To extend on the ideas of that work, we analyze here the effect of boundaries on the transverse Anderson localization of light in 2D photonic lattices of finite size; specifically near the lattice edges and corners. We assume that the lattice is optically induced in a nonlinear medium with saturable, photorefractive nonlinearity, in which strength is monitored by a single coupling parameter. A systematic quantitative study of dependence on the degree of disorder is presented here and, in addition, we focus on the photorefractive nonlinearity, where these effects have not yet been discussed. We reveal that the character of localization near the boundaries is in fact nontrivial, depending on both the strength of disorder and on the geometry of the surface. While one might expect that a surface, representing a major defect in the lattice akin to a defect or domain wall, should advance localization, this actually is not so. Both corners and edges effectively suppress Anderson localization, so that stronger disorder is needed near the boundaries to obtain the same localization effect as in the bulk. This surprising result is nonetheless consistent with the experimental observations reported earlier for one-dimensional lattices [9]. We further observe that the suppression is more pronounced at the corners, relative to the edges. However, depending on the nonlinear-medium characteristics, we discover that this is not always so: In Kerr-like media at lower levels of disorder, suppression is more pronounced at the edges than at the corners.

This paper is organized as follows. In Sec. II we introduce our model, which describes the propagation of light in a saturable nonlinear medium with an induced (regular or randomized) periodic potential. Section III summarizes our main results, and we discuss a number of effects depending on the variation of the lattice and nonlinearity parameters. Finally, Sec. IV concludes the paper.

II. MODELING DISORDER

We study localization of light in optically induced photonic lattices and describe the propagation of an optical beam along the z axis using the effective nonlinear Schrödinger equation for the electric-field amplitude F [10],

$$i\frac{\partial F}{\partial z} = -\Delta F - \Gamma F\frac{|F|^2 + V}{1 + |F|^2 + V}, \tag{1}$$

where Δ is the transverse Laplacian, Γ is the dimensionless coupling constant, and V is the transverse lattice potential. Nonlinearity is assumed to be of a saturable type, allowing an easy extrapolation to the Kerr regime, or to the regime of a strong lattice. A scaling, $x/x_0 \to x$, $y/x_0 \to y$, $z/L_D \to z$, is utilized for the dimensionless equation, where x_0 is the typical full width at half maximum (FWHM) beam waist and L_D

is the diffraction length. Intensities are given in units of the background light intensity. The propagation equation is solved numerically by employing a numerical approach developed earlier [11,12].

To study Anderson localization effects, we introduce disorder by using random potential V_d and choosing $V = V_p + rV_d$, where V_p is the perfect periodic potential describing a square lattice, and r $(0 < r < 1)$ is a deterministic real parameter that controls the degree of disorder in the lattice. Random potential is generated by multiplying V_p at each (x,y) point by a pseudo-random-number of uniform distribution; this ensures that V_d is not varied along the propagation direction. In this manner, one is actually dealing with the transverse Anderson localization [2,7]. We keep the input peak amplitude of the random potential V_{d0} equal to the input peak amplitude of the periodic potential V_{p0}, so that the strength of disorder relative to the periodic potential is controlled by a single parameter r. The degree of disorder is increased by increasing parameter r. Multiplying V_p by a pseudo-random-number is one way to introduce disorder; the other way is to randomize the distances between the lattice sites. The most general way is to combine both.

In simulations, we use experimental data for optically induced photonic lattices generated experimentally [13]: 10-mm-long Ce:SBN crystal and lattice spacing $d = 23$ μm. However, we vary the coupling constant Γ and the input beam intensities. We stress the fact that our findings apply to experimentally accessible systems. We use a square photonic lattice, but expect similar conclusions to hold for a hexagonal lattice (Ref. [2]) as well. The only difference would be the possibility of having two different corner geometries in the hexagonal lattice: at 60° and at 120°. For this case, we expect that a stronger disorder is needed for the "corner 60" geometry to obtain the same localization as for the "corner 120" geometry.

III. LOCALIZATION IN BULK, AT CORNERS, AND NEAR EDGES

A. General

We investigate localization effects near the edge and in the corner of a disordered, optically induced photonic lattice, and compare them with the localization in bulk lattice. By increasing the level of disorder, we observe the effect of Anderson localization, with the typical results summarized in Figs. 1(d)–1(f) for 60% of disorder ($r = 0.6$). For comparison, the corresponding cases without disorder are shown in Figs. 1(a)–1(c).

For quantitative analysis, we utilize the standard quantities used in the description of Anderson localization: the inverse participation ratio,

$$P = \int I^2(x,y,L)dxdy \left\{ \int I(x,y,L)dxdy \right\}^{-2}, \qquad (2)$$

and the effective beamwidth $\omega_{\text{eff}} = P^{-1/2}$ [2]. Since Anderson localization is essentially a statistical phenomenon, many realizations of disorder are needed to measure ensemble averages for the quantities of interest. Here, different disorder realizations are realized by starting each simulation with different seeds for a random-number generator. Even though different realizations lead to different transverse distributions of the probe beams, the measured values of P and ω_{eff} stay close to each other, as displayed by the error bars in Fig. 2 and Fig. 4.

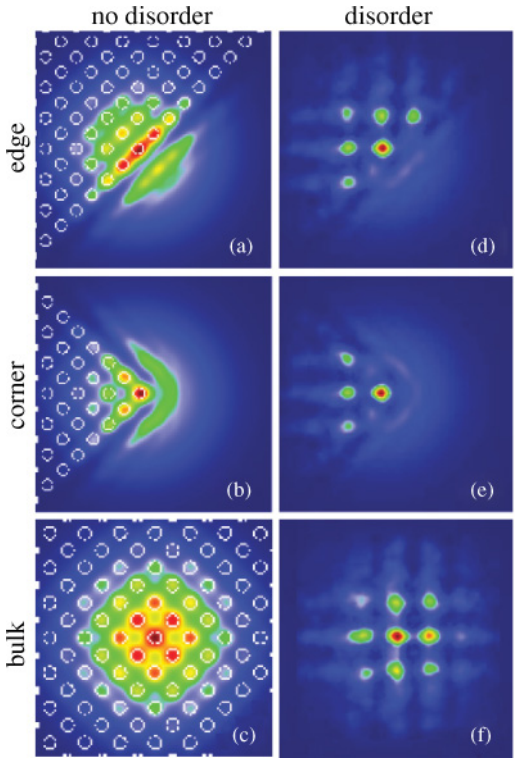

FIG. 1. (Color online) Anderson localization in a square photonic lattice. Localized modes are shown in (a)–(c) for no disorder, and in (d)–(f) for 60% disorder: (a,d) near the edge, (b,e) in the corner, and (c,f) in the bulk. Input beams are centered on the lattice site. The layout of lattice beams is shown in the first column by open circles. Physical parameters are $\Gamma = 7$, input beam intensity $|F_0|^2 = 0.1$, $V_{p0} = V_{d0} = 1$, and input beam FWHM $= 5d$.

The other quantity of interest for the description of Anderson localization is the localization length ξ. We find localization length by fitting the averaged intensity profile to an exponentially decaying profile $I \sim \exp(-2|r|/\xi)$. In our system, the localization length is given by $\xi = l^* \exp(k_\perp l^*/2)$, where l^* is the mean free path and $k_\perp = 2\pi/\omega_0$ is the transverse wave number, while ω_0 is the input beam FWHM. Here $\omega_0 = 115$ μm. We find that the localization length for the edge localization with 60% disorder level equals $\xi = 15.4$ μm, so that the mean free path is calculated to be 11.3μm.

B. Kerr vs saturable medium

It is of interest to consider the localization effects in different limits of the model. This is accomplished by varying the input peak amplitude of the lattice potential. Figure 2 presents the averaged effective width at the lattice output as a function of the disorder level for three different values of the lattice potential. The first case is for a weak lattice potential, the second is for the lattice peak intensity equal to the background intensity, and the third is for a stronger lattice

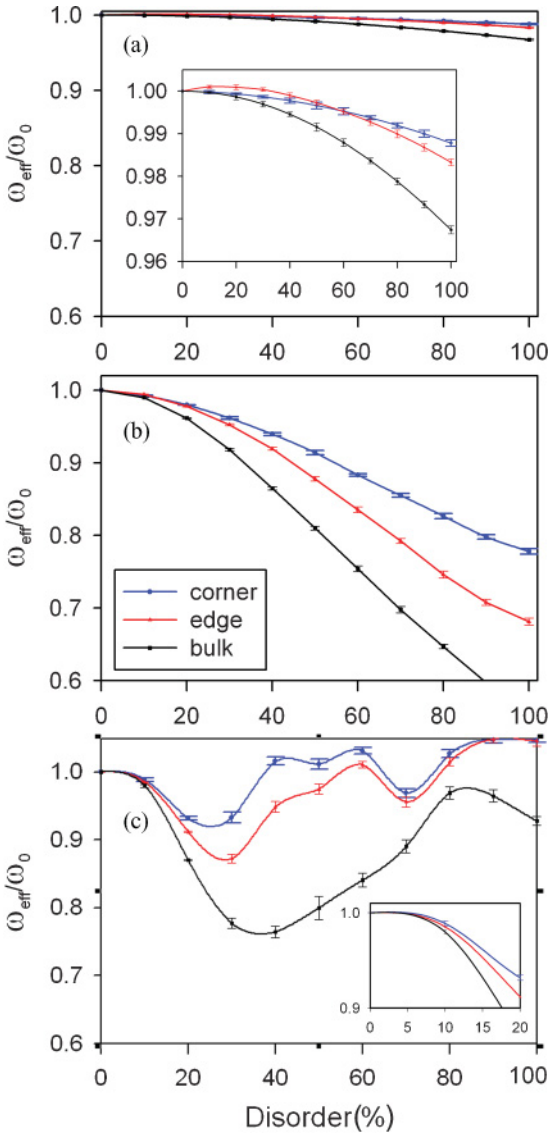

FIG. 2. (Color online) Effective beamwidth at the lattice output vs the disorder level for the edge, corner, and bulk modes. The widths are normalized to the input values. Error bars depict the spread in values coming from statistics. Insets in (a) and (c) display in more detail the regions of low disorder and high effective widths. (a) Weak potential $V_{p0} = V_{d0} = 0.1$, (b) $V_{p0} = V_{d0} = 1$, and (c) strong potential $V_{p0} = V_{d0} = 5$. Other parameters are as in Fig. 1.

potential. All the cases are for three different locations in the lattice. The averaged effective widths in Fig. 2 are taken over 50 realizations of disorder for each disorder level. Different realizations mean different seeds for a given random-number generator.

The effective beamwidth decreases as the level of disorder is increased, displaying a similar tendency as in the experiment [2]. It should be stressed that the effective beamwidth decreases faster in the bulk lattice as compared to the boundary, as the level of disorder is increased. Clearly, the beam propagation in the corner displays the least localization, followed by the beam at the edge. Interestingly, for lower disorders (up to about 50%) the localization in the corner is slightly more pronounced than the localization at the edge. The effect is more noticeable

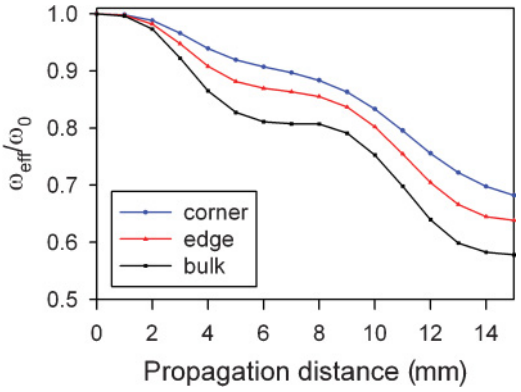

FIG. 3. (Color online) Influence of the crystal length on the localization. Effective beamwidth vs the propagation distance is shown for 60% disorder level. Other parameters are as in Fig. 1.

in the Kerr-like regime, when the input beam intensity and the input lattice potential are small compared to the background intensity [Fig. 2(a)]. As the lattice intensity is increased, the effect is washed away [Fig. 2(c)]. The phenomenon is probably due to the increased ability for light localization near the fixed lattice imperfection at low levels of disorder. At higher levels of disorder, this ability is diminished.

Figure 2(c) shows very interesting behavior in strong lattices. Effective beamwidths cease decreasing uniformly and develop minima in all the cases at disorder levels of ∼20%–40%; they then recover. There is another dip at ∼70% for the corner and edge modes, but these modes in general display little localization at very high levels of disorder, if at all.

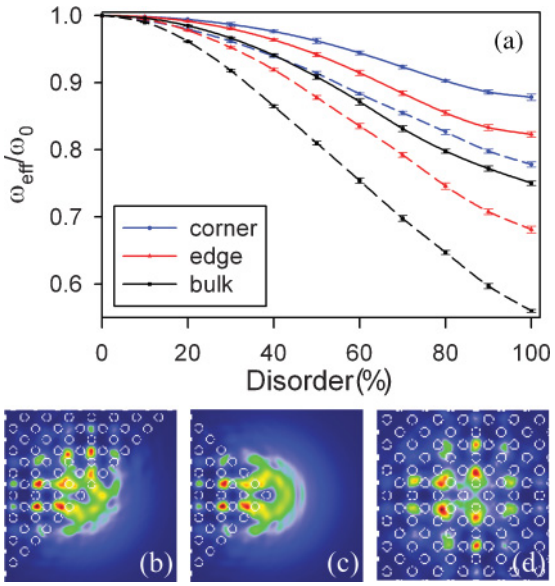

FIG. 4. (Color online) Focusing vs defocusing localization. (a) Effective beamwidth vs the disorder level. Focusing (dashed lines) and defocusing (solid lines) cases are compared for different levels of disorder. The corresponding localized modes are shown for 60% disorder level (b) near the edge, (c) in the corner, and (d) in the bulk. Parameters are as in Fig. 1, except for the negative $\Gamma = -7$.

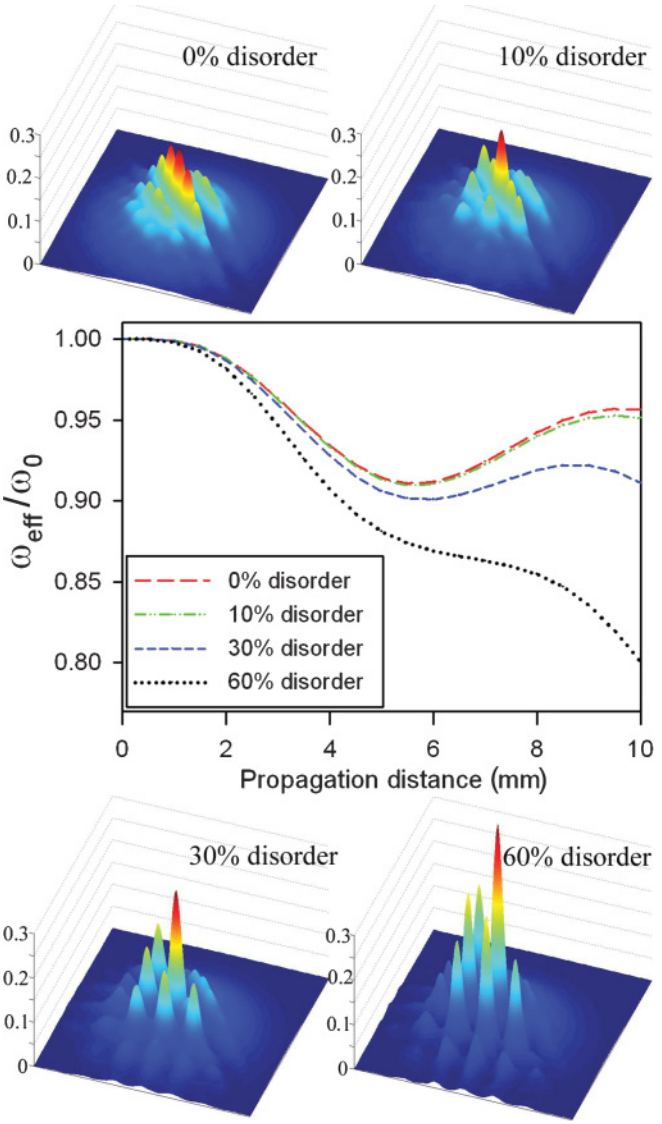

FIG. 5. (Color online) Effective beamwidth vs the propagation distance for different percentages of disorder. The four 3D intensity plots show the corresponding edge modes at the lattice output.

C. Size effects

Next, we investigate the size effects—the influence of the crystal length and the beam FWHM on the beam localization. Again, we consider three different locations in the lattice. Figure 3 presents the normalized effective beamwidth vs the propagation distance. Localization is more pronounced for longer propagation distances, i.e., for larger crystal lengths. Also, increasing the strength of nonlinearity makes localization more pronounced. These two parameters, coupling constant and propagation distance, produce similar effects on the localization. We also consider different input beam FWHM (not shown). For all three cases, the localization is more pronounced for broader beams.

D. Focusing vs defocusing case

We also look into the case with negative coupling constant Γ, i.e., localization with defocusing nonlinearity. Figure 4(a) presents the normalized effective beamwidth as a function of disorder, for both the focusing (dashed lines) and the defocusing (solid lines) localization. It is noted that the effective beamwidth decreases faster for the focusing case as compared to the defocusing case, as the level of disorder is increased. Typical localized modes for all three defocusing cases are presented in Figs. 4(b), 4(c), and 4(d); these should be compared with the corresponding modes in Fig. 1.

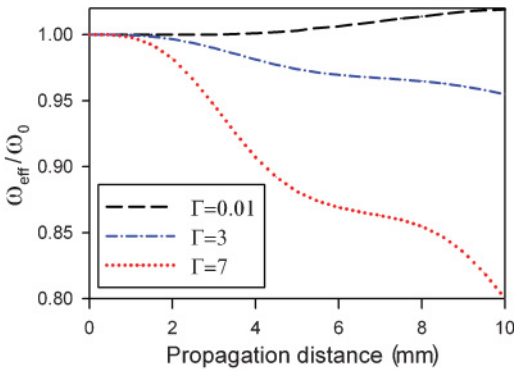

FIG. 6. (Color online) Comparison between the linear and nonlinear localization of the edge modes. Effective beamwidth is shown vs the propagation distance for different coupling constants. Other parameters are as in Fig. 1.

E. Edge localization

At the end, we concentrate on the localization near the edges. We study first the effective beamwidth as a function of the propagation distance (Fig. 5, middle panel) for different levels of disorder. We observe that the beamwidth displays self-focusing oscillations, which are less pronounced as the level of disorder is increased. No initial diffusive broadening is observed, since we are in the strongly nonlinear regime of the saturable model. In the upper and lower rows of Fig. 5, we show the edge modes at the lattice output as three-dimensional intensity distributions for different levels of disorder. Strong localization is evident. Still, a higher level of disorder is needed to observe similar localization near the edge, as compared to the bulk.

Finally, we analyze the effect of nonlinearity on the beam localization for a fixed level of disorder (in the case shown, 60%). To compare with the linear propagation in a disordered lattice, we reduce the nonlinearity by decreasing the coupling constant Γ to 0.01. Figure 6 shows that the effective beamwidth decreases faster as the nonlinearity strength is increased; this tendency is expected. Similar results, consistent with the ones reported in the earlier experiments [2,3], are obtained when one moves into the Kerr regime; this is achieved by assuming that the lattice and the beam intensities are small relative to the background intensity [which is taken to be 1 in Eq. (1)].

IV. CONCLUSIONS

We have analyzed numerically how the edges and corners of truncated two-dimensional photonic lattices modify the phenomenon of Anderson localization of light. We have demonstrated that the effect is nontrivial, and that it depends on the strength of disorder and the characteristics of the

nonlinearity model. For weak disorder, the presence of a corner slightly enhances light localization relative to the edge, due to the ability to better localize light near the lattice imperfection. For strong disorder, both corners and edges effectively suppress Anderson localization, so that a higher level of disorder near the boundaries is required to obtain similar localization as in the bulk; Anderson localization in the corner is less effective than the localization at the edge.

ACKNOWLEDGMENTS

This work was supported by the Ministry of Science and Technological Development of the Republic of Serbia (Project No. OI 171036), the Qatar National Research Foundation (NPRP Project No. 25-6-7-2), and the Australian Research Council. D.M.J. would like to thank the Alexander von Humboldt foundation for the Fellowship for Postdoctoral Researchers.

[1] *50 Years of Anderson Localization*, edited by E. Abrahams (World Scientific, Singapore, 2010), pp. 597.

[2] T. Schwartz, G. Bartal, S. Fishman, and M. Segev, Nature (London) **446**, 52 (2007).

[3] Y. Lahini, A. Avidan, F. Pozzi, M. Sorel, R. Morandotti, D. N. Christodoulides, and Y. Silberberg, Phys. Rev. Lett. **100**, 013906 (2008).

[4] J. Billy, V. Josse, Z. Zuo, A. Bernard, B. Hambrecht, P. Lugan, D. Clément, L. Sanchez-Palencia, P. Bouyer, and A. Aspect, Nature (London) **453**, 891 (2008).

[5] S. Flach, D. O. Krimer, and Ch. Skokos, Phys. Rev. Lett. **102**, 024101 (2009).

[6] C. Conti and A. Fratalocchi, Nature Phys. **4**, 794 (2010).

[7] H. De Raedt, A. Lagendijk, and P. de Vries, Phys. Rev. Lett. **62**, 47 (1989).

[8] D. M. Jović and M. R. Belić, Phys. Rev. A **81**, 023813 (2010).

[9] A. Szameit, Y. V. Kartashov, P. Zeil, F. Dreisow, M. Heinrich, R. Keil, S. Nolte, A. Tünnermann, V. A. Vysloukh, and L. Torner, Opt. Lett. **35**, 1172 (2010).

[10] M. Belić, Ph. Jander, A. Strinić, A. Desyatnikov, and C. Denz, Phys. Rev. E **68**, 025601 (2003).

[11] M. R. Belić, J. Leonardy, D. Timotijević, and F. Kaiser, J. Opt. Soc. Am. B **12**, 1602 (1995).

[12] M. Belić, M. Petrović, D. Jović, A. Strinić, D. Arsenović, K. Motzek, F. Kaiser, Ph. Jander, C. Denz, M. Tlidi, and P. Mandel, Opt. Express **12**, 708 (2004).

[13] X. Wang, A. Bezryadina, Z. Chen, K. G. Makris, D. N. Christodoulides, and G. I. Stegeman, Phys. Rev. Lett. **98**, 123903 (2007).